Available online at www.sciencedirect.com

ScienceDirect

Procedia Engineering 00 (2017) 000–000

Procedia Engineering

www.elsevier.com/locate/procedia

14th Hypervelocity Impact Symposium 2017, HVIS2017, 24-28 April 2017, Canterbury, Kent, UK

Challenges of Debris-Impact Risk Assessment for Robotic Spacecraft

James Chinn[a,*], Martin Ratliff[a]

[a]*Jet Propulsion Laboratory, California Institute of Technology, 4800 Oak Grove Drive, Pasadena, CA 91109, USA*

Abstract

This paper describes an orbital debris impact risk assessment performed on the command and data subsystem electronics box of QuikSCAT, a functioning spacecraft with approximately 18 years on orbit. Several aspects of the analysis are paid particular attention. First is the modeling of a thermal blanket at a small stand-off distance from the box chassis. The properties of the blanket are such that under some assumptions, it may be treated as an effective bumper shield, and under other assumptions, it may not. The assumptions and their effects on the results of the analysis are explored. Similarly, the configuration of the electronic components inside the chassis are such that several definitions of failure criteria appear plausible. The results of each treatment are presented together and compared with the status of the actual electronics box. The failure predictions vary widely between treatments, and the more conservative assumption sets predict incredulously high probabilities of failure. This is problematic because the conservative assumptions are the ones typically used in analyses for flight projects.

Peer-review under responsibility of the scientific committee of the 14th Hypervelocity Impact Symposium 2017.

Keywords: Orbital Debris; MMOD; risk; assessment; Bumper; ORDEM; QuikSCAT

* Corresponding author. Tel.: +1-818-354-9459; fax: +1-818-393-4699.
E-mail address: James.Z.Chinn@jpl.nasa.gov

Peer-review under responsibility of the scientific committee of the 14th Hypervelocity Impact Symposium 2017.

1. Introduction

The design of an Earth-orbiting spacecraft typically addresses the risk of sustaining critical damage from orbital debris. Several tools and damage predictor equations are available to calculate this risk for common configurations. However, shield geometries are frequently encountered that do not fit the characteristics of the data set from which the tools were derived. This adds uncertainty to the analyses, which one is tempted to bound using conservative assumptions. As will be shown in this paper and as often encountered by the authors, bounding the uncertainty in the analysis can lead to an impractically large range of failure probabilities, and conservative assumptions often lead to incredulously high probabilities of failure. To make these analyses more useful, new data sets or new methods of applying the current data sets with more confidence to a wider range of common configurations is desirable. Of particular interest to the authors in their work on robotic missions at JPL are methods of handling Multi-Layer Insulation (MLI) as a bumper shield, of interpreting damage to electronics behind a double wall configuration, and of predicting shield response to steel and copper projectiles.

To illustrate the problem, an analysis of a spacecraft electronics box is presented in this paper. The spacecraft is QuikSCAT, which has been in orbit for approximately 18 years, and the subject electronics box is known to still be fully operational. The effects of several assumptions are investigated. First, the effect of assuming that MLI functions as the first wall, or bumper shield, of a double-wall shield configuration is explored, demonstrating the difficulties of modifying Ballistic Limit Equations (BLEs) to handle marginal shields. Second, the effect of discounting some of the box perforations based on the configuration of the circuit board inside the box is explored. The most conservative treatments predict an extremely high probability of failure, which is difficult to believe given the electronics' functional status. The most optimistic treatment predicts a believable probability of failure. The correct probability of failure ostensibly lies somewhere between the two numbers, but where is uncertain. This is problematic because the difference between the conclusions of the two treatments is so large that it is difficult to say with confidence anything useful about the probability of survival of the electronics box. This problem is not unique to the subject analysis; it is frequently encountered by the authors during their analyses of JPL spacecraft.

2. QuikSCAT Spacecraft

The intent of the analysis was to compare the actual status of a piece of flight hardware to the prediction of the hardware's survival in the debris environment. The spacecraft chosen for this analysis was QuikSCAT (Figure 1). QuikSCAT is an Earth observation satellite whose primary mission was to measure surface wind speed and direction over global oceans using JPL's SeaWinds instrument. QuikSCAT was manufactured by Ball Aerospace & Technologies, and launched in 1999. The science instrument failed in 2009, but the engineering subsystems are currently still functional. QuikSCAT mission parameters are shown in Table 1.

The most appealing aspect of QuikSCAT from an analyst's perspective is the presence of electronics boxes that are directly exposed to orbital debris. This allows for relatively straightforward orbital debris damage analysis.

Figure 1. Artist Depiction of QuikSCAT [1]

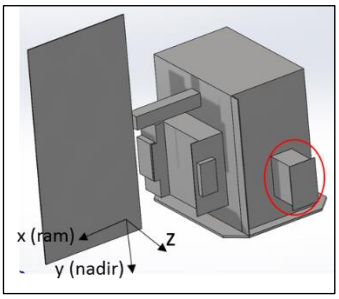

Figure 2. CAD Model of QuikSCAT. CDS Circled in Red.

Table 1. QuikSCAT Mission Parameters

Parameter	Value
Launch Date	June 19, 1999
Perigee (km)	802.5
Apogee (km)	803.9
Inclination (deg)	98.6
Orbit Type	Sun-Synchronous
Target	Earth
Primary Instrument	SeaWinds (JPL)
Manufacturer	Ball Aerospace
Primary Mission Length	10 years, 4 months
Secondary Mission Length	Ongoing

3. Model

The Bumper3-lite code, developed by the hypervelocity impact group at NASA, was used to calculate the probability of perforating the electronics box chassis. As input, the code requires a debris flux, finite element mesh of the spacecraft, shield geometry, and material properties. It then calculates the number of failures of each surface, accounting for directionality and shadowing of the debris flux by one part of the spacecraft to another.

To define the orbit, a Two Line Element (TLE) was obtained for QuikSCAT. The TLE was acquired from CelesTrak, a website maintained by The Center for Space Standards and Innovation [2]. It was input into the current NASA orbital debris model, ORbital Debris Engineering Model v.3 (ORDEM3), to generate the orbital debris environment for the trajectory. The environment covered a 15-year span from Jan 1 2000 to Dec 31 2014, representing most of QuikSCAT's mission duration to date. The release version of ORDEM3 only calculates fluxes back to 2010. Mark Matney at the NASA Orbital Debris Program Office provided QuikSCAT's ORDEM3 environment from 2000-2010.

Several electronics boxes were considered for this analysis. The selection criteria were that the box lent itself to a relatively straightforward analysis and that its functional status was known (functioning or not functioning). Specifically, it was desired that any wall on the box seeing significant debris had a simple single or double wall shielding configuration, and that the electronic components behind those walls were such that there could be deduced a simple correspondence between number of perforations and number of failures. Six boxes were considered (observable in Figure 1), out of which one fit the selection criteria. This box was the Command and Data Subsystem (CDS), circled in Figure 2. The CDS is responsible for several functions on QuikSCAT, including sequence storage, spacecraft clock, telemetry packaging and coding, data storage, and fault protection. The unit is mounted on the port side of the spacecraft and consists of an aluminum chassis containing many circuit boards. The circuit boards are all connected to a backplane electronics bus board, which is parallel to and immediately interior to the +X (ram-side) box wall (Figure 3). MLI covers every exposed face of the box aside from the +Z (port-side) face, which functions as a radiator. The CDS was is known to still be functioning [8].

There was no available CAD model of QuikSCAT, but there were engineering drawings of most of the spacecraft. From these drawings, a CAD model of the spacecraft with approximate dimensions was generated (Figure 2). Only the components relevant to the analysis were included. This consisted of the CDS box and any part of the structure that would provide shadowing to the CDS from the debris environment (at the time the model was created, one other box was still being considered and is also included). From the CAD model, a finite element mesh of the spacecraft was generated. This mesh was imported into the impact analysis software, Bumper3-lite.

4. Analysis Inputs

The orbital debris environment as defined in ORDEM3 consists of several particle populations. All were considered in the analysis, but two populations contribute nearly all (>99%) of the perforations. These will be referred to as the Medium Density (MD) population, which consists of aluminum particles and has an assigned density of 2.8 g/cm^3, and the High Density (HD) population, which consists of steel and copper particles and has an assigned density of 7.9 g/cm^3. In the orbit of QuikSCAT, the majority of particles will impact the spacecraft nearly

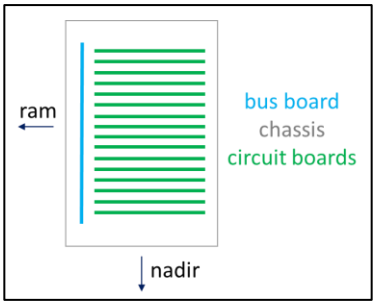

Figure 3. CDS Configuration

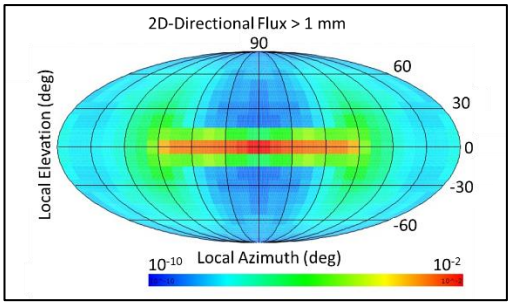

Figure 4. Distribution of Flux by Elevation and Azimuth

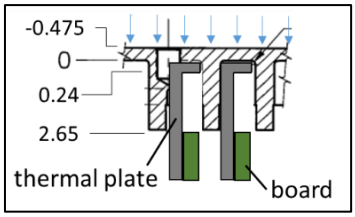

Figure 5. Cross Section of Port Side Chassis Wall, Units: cm

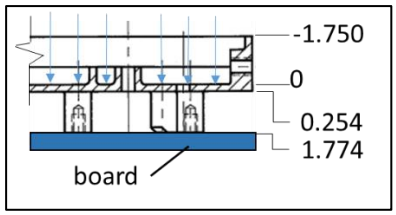

Figure 6. Cross Section of Ram Side Chassis Wall, Units: cm

head-on relative to the spacecraft velocity vector at approximately 15 km/s. The distribution of flux (1 mm and larger particles in all populations) by spacecraft elevation and azimuth is shown in Figure 4. The flux is almost entirely concentrated in the x-z plane of the spacecraft (see Figure 2 for the spacecraft coordinate system). Most debris is encountered in the ram direction, decreasing towards port and starboard, and becoming effectively zero in the wake direction. The debris flux decreases rapidly towards the nadir and zenith directions, again becoming effectively zero at the extremes. Therefore, the ram- and port-facing sides of the CDS dominate the unit's risk of damage from debris, and were the only two sides analyzed further.

A cross sectional diagram of the port chassis wall is shown in Figure 5. The wall functions as a radiator and is slotted to accommodate circuit boards. Each board has a thermal plate to facilitate heat transfer to the radiator. This is an aluminum plate on which each board is mounted. The plate extends around the boundary of the board and interfaces with the radiator wall as shown in the cross section in Figure 5. The boards themselves are mounted to the thermal plates below the edge of the interface, indicated by the 2.65 cm mark in Figure 5. Debris impacting this port-side wall will at minimum have to perforate 0.715 cm of aluminum before reaching any sensitive electronics, and for most of the wall area, will have to perforate up to 3.125 cm of aluminum. In addition, because it is the port side, most debris, and the most energetic debris, will impact at fairly high angles of incidence, decreasing their penetrating capability. Compared to the ram side (discussed in the next paragraph), the port side of the CDS was expected to contribute a negligible number of perforations. As such, it was not analyzed further.

A cross sectional diagram of the ram chassis wall is shown in Figure 6. The bulk of the wall is 0.254 cm of aluminum thick and the bus board is 1.52 cm behind it. Not shown in the figure is a layer of MLI. The MLI has 2 layers of 8 mil Beta Cloth and an areal density of 0.079 g/cm^2. The MLI is spaced off the chassis wall by 1.75 cm.

5. Analysis

As will be shown, the specs for the MLI on the CDS give it marginal performance as a bumper shield. Therefore, two treatments will be considered: one optimistic approach where the MLI is treated as a bumper shield, and one conservative approach where it is treated as supplemental to a single wall shield configuration. Ballistic limit equations have been developed for some configurations of MLI as a bumper shield [3], but these were developed for constructions with larger areal densities (0.188 g/cm^2 and 0.307 g/cm^2) and are not applicable in this situation.

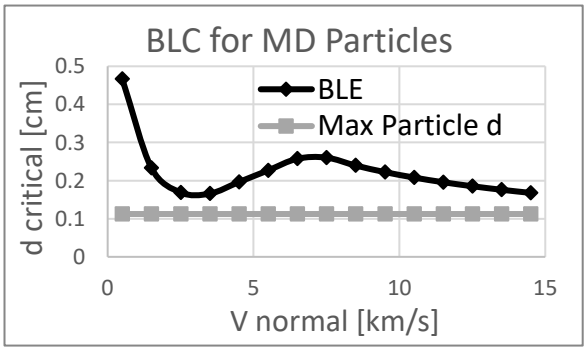

Figure 7. MD Ballistic Limit Curve and Max Particle Diameter

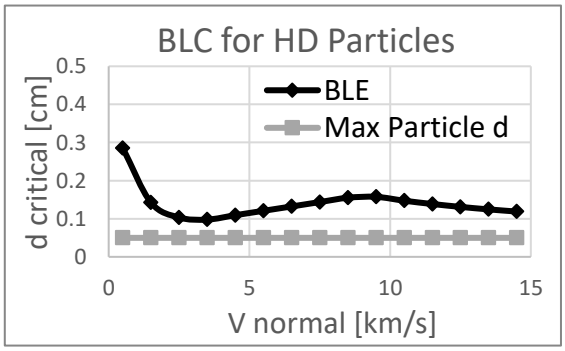

Figure 8. HD Ballistic Limit Curve and Max Particle Diameter

Another common method used to model MLI as a bumper is to convert its areal density to an equivalent aluminum thickness and proceed with the standard Christiansen NNO double wall BLE for aluminum debris impacting an aluminum shield [4]. This treatment is laid out in the following paragraphs, after which the assumptions necessary to carry it out are scrutinized.

The MLI has an areal density of 0.079 g/cm^2, which is equivalent to 0.029 cm of aluminum. Therefore, the equivalent double wall configuration consists of a 0.029 cm aluminum bumper, 1.75 cm spacing, and 0.254 cm aluminum rear wall. The BLEs that describe this shield's response to MD and HD particles are plotted as black lines in Figures 7 and 8. The line specifies the maximum diameter particle the shield will defeat for a given velocity.

As described in [4], one of the conditions that must be met to avoid under-predictions by the BLE is that the bumper thickness must exceed a threshold thickness t_b:

$$t_b \geq c_b * d * \left(\frac{\rho_p}{\rho_b}\right) \quad (1)$$

Where d is the diameter of the perforating particle, ρ_p is the density of the particle, ρ_b is the density of the bumper, and c_b is a coefficient dependent upon the ratio of the spacing (S) to perforating particle diameter. The criteria listed in [4] is that $c_b = 0.25$ when $S/d < 30$ and $c_b = 0.2$ when $S/d \geq 30$. In the configuration being addressed, S = 1.75 cm, and d is given by the BLEs in Figures 7 and 8. For all velocities at which the bumper may break up a particle (approximately > 3 km/s), for and both particle types, $S/d < 18$. Therefore, $c_b = 0.25$ is used in Equation 1.

Rearranging Equation 1, one can solve for the maximum diameter particle for which the BLE is reliable. For the current shielding configuration, the maximum diameter Medium Density particle for which the BLE will reliably predict failure is 0.1124 cm; for High Density particles, the maximum diameter is 0.0498 cm. These two values are plotted in grey in Figures 7 and 8. For a shield functioning according to the specifications laid out for the NNO BLE in [4], the grey line would be above the black line in the hypervelocity region: Vn ≥ 7 km/s in the MD plot and Vn ≥ 9 km/s in the HD plot. Because it is not, the NNO BLE may over-predict the shielding ability of this configuration.

Reimerdes et al proposed a modification to the Christiansen BLE to handle thin bumpers [5]. For the hypervelocity region, the modification is based on tests of Cadmium projectiles and shields, and on simulations of aluminum projectiles and shields [6]. As t_b/d decreases below the threshold specified in the NNO BLE, the ballistic limit decreases as well. In other words, for any velocity at which the grey line is below the black line (all velocities in this case), the "d critical" value of the black line at that point will decrease by an amount specified in the Reimerdes modification, dependent upon how far below the black line the grey line is.

The Reimerdes equation is not implemented in the version of Bumper3 available to the authors. As such, the Reimerdes modification was used in several specific hand calculations to estimate the degraded shield performance. The goal was to create a coarse approximation of the ballistic limit curve. To do this, the velocity range was truncated at 14.5 km/s. By examination of the ORDEM3 environment, there are no significant particle contributions with normal impact velocities above 14.5 km/s. Next, possible locations for global minima and maxima were identified on the curve. The minima are indicated by blue circles in Figure 9 and the velocity of the one local maximum (excluding the 0 km/s boundary) is indicated by the vertical blue line at the hypervelocity transition point.

There are two points on the Reimerdes ballistic limit curve at which the minimum critical particle diameter may exist. These are the maximum velocity, 14.5 km/s in this case, and the shatter velocity. The shatter velocity is the point at which the pressures induced in the particle upon impact with the bumper begin to break the particle apart. The maximum velocity is the right-most circle in Figure 9 and the shatter velocity is the left-most circle in Figure 9. From the shatter velocity, the critical particle diameter increases with velocity in both directions, and from the maximum velocity, the critical particle diameter increases toward lower velocities. The local maximum between the two points occurs at the hypervelocity transition region, which is 7 km/s for Medium Density particles and 9 km/s for High Density particles (again, indicated by the blue vertical line in Figure 9).

This is the general form the ballistic limit curve takes, but the minima and maximum can shift along both axes. In order to bound the curve, the critical diameters at the minima must be calculated, and the velocity corresponding to the maximum must be identified. The critical diameters at the two minima were calculated using the Reimerdes modification, and the maximum occurs at the hypervelocity transition, which is known to be 7 km/s for MD particles and 9 km/s for HD particles. Using these values, a crude bound on the Reimerdes BLE can be

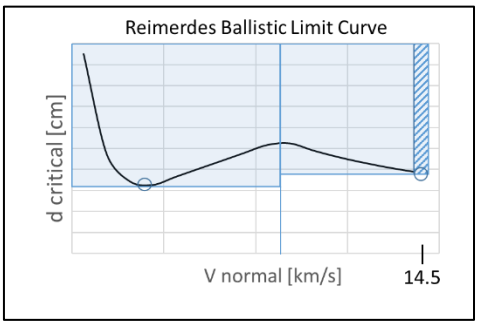

Figure 9. Coarse Approximation of Reimerdes Ballistic Limit Curve

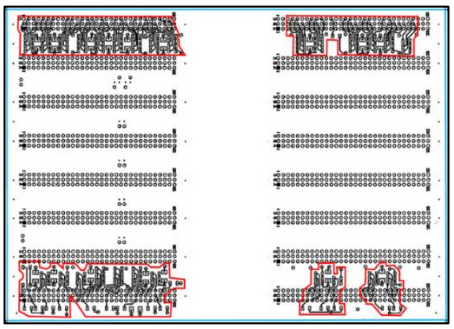

Figure 10. Most Superficial Layer of CDS Backplane; Blue Area Defines the Perimeter of the Plane and Red Areas Define Areas most Vulnerable to Impact from Penetrating Debris

made. The bounded region is indicated by the two light blue shaded regions in Figure 9. The shaded regions together represent a restricted particle set that is still guaranteed according to the BLE to include all potentially relevant particles (i.e. those particles that may fail the shield).

What is useful about creating this set of particles is that one particularly large contributor can be identified. This contributor consists of the particles that impact with a normal velocity between 14 and 14.5 km/s (the darker hashed region in Figure 9). Using Bumper3 and the critical diameter calculated by the Reimerdes modification for 14.5 km/s, the number of these particles was calculated. In the MD case, there are 0.05 of these particles, making up 73% of all the impacts in the light blue regions, and in the HD case, there are 1.33 of these particles, making up 81% of all the impacts in those regions. Taking into account that these regions include some particles that will not fail the shield (those in the blue region but below the black curve in Figure 9), the 73% and 81% cited actually account for *at least* 73% and 81% of all shield failures according to the Reimerdes BLE. Combining the MD and HD results, there are between 1.38 and 1.38 ÷ 81% = 1.70 shield failures predicted in this treatment of the problem.

There are several assumptions made in this treatment that are not necessarily valid. The first is the use of MLI as a bumper shield in place of aluminum. The tests used to generate the Christiansen NNO BLE used aluminum bumpers, and extrapolation to a multi-layered bumper made of non-aluminum materials is not necessarily valid. Similarly, the Reimerdes modification is based on cadmium bumper tests and aluminum bumper simulations, and extrapolation to multi-layer insulation is not necessarily valid [6]. The second is the use of the Christiansen NNO BLE and Reimerdes Modification to model the response to high density (steel and copper) projectiles. Yet again, the BLEs were not formulated on data or simulations involving these materials. Lastly, the spacing in this configuration may be smaller than adequate for proper performance of the NNO BLE. The minimum recommended S/d ratio, specified in [4], is 15. The subject configuration has 1.75 cm spacing and critical projectile diameters of 0.119 cm and 0.168 cm for 14.5 km/s HD and MD particles, respectively (before Reimerdes modification). These are S/d ratios of 14.7 and 10.1. The value for HD is marginal, and the value for MD is rather low, adding some uncertainty to the results. For the Reimerdes diameters, the ratios are improved to 21.6 and 10.9.

Because of these potentially invalid assumptions, a more conservative treatment is considered. This treatment assumes that the MLI does not behave like a bumper, and instead it is combined with the chassis wall as a single-wall shield geometry. BLEs have been developed for handling MLI on top of a single wall configuration [3]. This BLE is implemented in Bumper3 and was run for the subject configuration: 0.254 cm Al rear wall with 0.079 g/cm^2 MLI. This shield experiences 11.3 failures from perforations only and 14.85 failures including detached spalls. These are much higher numbers than the 1.38 - 1.70 failures predicted using the Reimerdes double wall calculation.

6. Failure Criteria

There are commonly two ways to define failure of an electronics box due to orbital debris impact. One is perforation of the box. A particle that perforates the box will send debris into the box, potentially damaging electronics. A more conservative approach is to include detached spalls along with perforations. The Christiansen

double wall NNO BLE always includes detached spalls along with perforations, but the single wall Cour-Palais BLE can distinguish between the two. Both will be considered.

In addition, it is not necessary that every failure of the chassis will lead to failure of the board. Putzar et al demonstrate this with their impact tests on a chassis containing a circuit board [7]. In the CDS box, the bus plane located behind the ram facing wall is a layered circuit board. The outward-facing side of the board is diagrammed in Figure 10. There are circuit elements on this layer within the red regions of the figure. The electronics are conformal coated so a short circuit induced by the vaporized chassis material is not deemed a plausible failure mode. Therefore, a direct impact from ejecta of a failed shield is assumed to be the only failure mode. The circuit elements occupy approximately 16% of the board area, and it is assumed that any direct impact to these elements will cause failure. Therefore, as a lower bound, 16% of shield failures are assumed to cause electronics failure. The many rows of circles shown in Figure 10 are solder points for connectors on the other side of the board. The chance that an impact could create a bridge to short two solder points together is unknown. In an optimistic treatment, they may be assumed to pose negligible risk. In a conservative treatment, some, if not all impacts to these areas should be considered failure. Below the layer shown in Figure 10 are several insulating layers, ground planes, and planes containing traces. Again, their response to an impact is not easily predictable. And again, in an optimistic treatment, this failure mode may be considered to pose negligible risk, while in a conservative treatment, this failure mode may be accounted for. Based on this assessment, two treatments of the board failure modes are considered. One is an optimistic analysis which takes 16% of box failures as board failures, and one is a conservative analysis which takes 100% of box failures as board failures. Ostensibly, the correct percentage is somewhere between these two numbers.

7. Results and Comments

The results of the analysis are shown in Table 2. The results change significantly depending upon which assumptions are used. The most optimistic approach, modeled as a double wall configuration with 16% lethal area, predicts 0.22 failures over 15 years, equivalent to a chance of failure of 20%. This is a plausible number considering that the CDS box is still functioning. As uncertainty in the analysis is bounded using conservative assumptions, the number of failures climbs. The most conservative approaches predict very incredulous probabilities of failure. The most conservative, a single wall configuration with 100% lethal area and detached spall failure mode, predicts 14.85 failures over 15 years, equivalent to a chance of failure >99.999%. While one would expect conservative assumptions to result in high predicted chances of failure, the most conservative cases seem to do so in excess.

The subject analysis is more detailed than a typical analysis. Effort was taken to modify the results of Bumper3 to handle a marginal MLI bumper, and to identify in detail the electronics within the CDS chassis and their vulnerability to debris. Generally, because there are many components to analyze on a spacecraft, there is neither time nor money to investigate the problem in such detail. Therefore, conservative assumptions are made to simplify the analyses. As evidenced in the subject paper, these assumptions can, and often do, lead to very high predicted probabilities of failure. This poses a problem during the design phase of a spacecraft because while a 60% chance of failure is believable given the status of a still-functioning spacecraft, a design with a 60% chance of failure is an unacceptable design. To handle this, conservative assumptions used in the analysis can be rolled back, but it is difficult to know which or how many to recall. This potentially leaves the spacecraft vulnerable to failures that the assumptions were intended to account for.

The MLI case investigated in the subject paper is a common one. Often on JPL spacecraft, MLI takes on a

Table 2. Number of Failures and Chance of Failure for Several Assumptions – Most Optimistic to Most Conservative

Assumptions	# Failures	% Chance of Failure
Double Wall and 16% Lethal Area - Detached Spall Failure (Most Optimistic)	0.22	20.0
Double Wall and 100% Lethal Area - Detached Spall Failure	1.38	74.8
Single Wall and 16% Lethal Area - Perforation Only Failure	1.81	83.6
Single Wall and 16% Lethal Area - Detached Spall Failure	2.38	90.7
Single Wall and 100% Lethal Area - Perforation Only Failure	11.30	99.999
Single Wall and 100% Lethal Area - Detached Spall Failure (Most Conservative)	14.85	99.999...

secondary function as a bumper shield. The performance of MLI as a bumper is not well characterized. As mentioned in the Analysis section, there are some cases where tests have been conducted, but their generalizability to other types of MLI isn't well studied, especially for MLI that may only function marginally as a shield.

As already mentioned, there have been some studies investigating the vulnerability of electronics within chassis [4], but the body of work isn't complete enough to claim much about a general case.

It is assumed in this analysis that the orbital debris environment, ORDEM3, is accurate. ORDEM3 has its own uncertainty, which will have a large effect on the subject analysis. It was desired to keep the present analysis focused on shielding and failure criteria, but for reference, a comparison with an older version of the environment definition was run. In the most conservative case (single wall, 100% lethal area, detached spall failure), an analysis using the ORDEM2k environment predicts 0.61 failures instead of 14.85 failures as predicted using ORDEM3. This drops the predicted chance of failure from over 99.999% to 45.7%.

It is also assumed that the BLE equations are applicable to the High Density steel and copper particles. While the BLEs do account for projectile density, steel and copper particles were not included in their test data sets. Therefore, additional uncertainty should be added to all the BLE predictions when analyzing the response to High Density projectiles.

8. Conclusion

The tools used to perform orbital debris impact risk assessments are based on tests conducted on particular geometries and particular materials. Often when performing impact risk assessments on spacecraft, configurations are encountered with geometries and materials that fall outside the set of those included in the tests. This makes the applicability of the tools more uncertain, which often results in several plausible treatments of the problem. The predicted chance of failure can vary significantly from treatment to treatment, and the most conservative analyses often predict incredulously high probabilities of failure. Optimistic assumptions become necessary to achieve reasonable risks, potentially leaving the spacecraft vulnerable to failure. To make these analyses more useful, new data sets or new methods of applying the current data sets with more confidence to a wider range of common configurations is desirable. Of particular interest to the authors in their work on robotic missions at JPL are methods for handling MLI as a bumper shield, for interpreting damage to electronics behind a double wall configuration, and for predicting shield response to steel and copper projectiles.

9. Acknowledgements

The research was carried out at the Jet Propulsion Laboratory, California Institute of Technology, under a contract with the National Aeronautics and Space Administration.

10. References

[1] Author Unknown, QuikSCAT, Winds QuikSCAT, NASA/JPL-Caltech, https://winds.jpl.nasa.gov/missions/quikscat/
[2] CelesTrak, http://www.celestrak.com/NORAD/elements/resource.txt
[3] E.L. Christiansen, J. Arnold, B. Corsaro, A. Davis, F. Giovane, J. Hyde, D. Lear, J.C. Liou, F. Lyons, T. Prior, M. Ratliff, S. Ryan, G. Studor, "Handbook for Designing MMOD Protection." NASA Johnson Space Center, NASA/TM-2009-214785, 2009.
[4] E.L. Christiansen. "Design and Performance Equations for Advanced Meteoroid and Debris Shields." Int. J. Impact Eng., 14:145–156, 1993.
[5] H.-G. Reimerdes, D. Nolke, F. Shafer, "Modified Cour-Palais/Christiansen damage equations for double-wall structures." Int Journal of Impact Engineering, 33: 645-654, 2006.
[6] Gehring, John W., Jr. "Theory of Impact on Thin Targets and Shields and Correlation with Experiment." Ed. Impact Physics Laboratory General Motors Corporation and AC Electronics Defense Research Laboratories. *High-Velocity Impact Phenomena*. Ed. Ray Kinslow and Department of Engineering Science, Tennessee Technological University. New York: Academic, 1790. 144-46. Print.
[7] R. Putzar et al, "Vulnerability of Spacecraft Electronics Boxes to Hypervelocity Impacts." IAC-05-B6.4.02.
[8] Personal Communication with Robert Gaston, QuikSCAT Project Manager.